Prediction of velocity and coat-weight limits based on filter-cake formation

Douglas W. Bousfield

ABSTRACT: A model is proposed to predict the maximum velocity at which a blade coater can operate before runnability problems occur. Many runnability problems seem to correlate with the dewatering of the coating. The model is based on fluid mechanics and considers the effects of (a) filter-cake formation on the sheet surface and (b) sheet roughness. The model shows that formation of a filter-cake can generate a large pressure pulse under the blade, which drives more fluid from the coating into the paper. The model predicts the maximum operating speed and the blade forces for a given coat weight and paper roughness. Comparison of model predictions with data from several researchers shows good agreement. The model provides a tool to optimize coating solids and web velocity for given coat-weight targets and paper properties.

KEYWORDS: Blade coaters, coating, coating weight, fluid dynamics, roughness, runnability, solids content, velocity, water removal.

The tradeoff between coating-suspension solids and coater speed is well known. Many coating suspensions perform well at one operating speed yet cause runnability problems at higher speeds. This can be a problem on coaters where high speeds are desirable to maximize capital investment.

Runnability problems at high speeds include coating scratches or streaks and blade deposits such as weeps, spits, whiskers, or stalagmites *(1)*. Coat-weight uniformity in the cross-machine direction (CD) also can be difficult to obtain. In some cases, speeds can be increased by lowering the solids content of the coating. However, lower solids reduce the coating quality and increase the energy cost to dry the coating *(2)*. In addition, high-solids coatings retain latex and pigments in the coating layer and prevent latex penetration into the web *(3, 4)*.

Bousfield is an associate professor in the Department of Chemical Engineering and the Paper Surface Science Program, University of Maine, Orono, ME 04469-5737.

High speeds and high solids are desirable for most mill operations. The solids should be as high as possible without causing runnability problems. However, most coatings have a speed limit, a maximum velocity at which the coating can be run. Taylor *(5)*, Gane *et al. (6)*, McGenity *et al. (7)*, and Tran *et al. (8)* provide data characterizing these speed limits for various solids levels. In most cases, the maximum speed decreases as solids increase.

The mechanism that limits coater speed is not understood at this time, even though coaters often operate near this limit. Formation of blade deposits is not restricted to high-solids, high-speed coating operations. Low temperatures and low blade angles also promote blade deposits *(6, 9)*. The influences of pigment shape, additives, and blade geometry on runnability also are not well characterized. In addition, the effects of sheet roughness and coating rheology on this speed limit are not understood. The result is that mills must rely on a trial-and-error approach to determine the maximum solids–velocity combination for any given coating–coater–paper combination. Experiments to determine these limits are expensive.

Dilatant or shear-thickening rheology has been identified by Taylor *(5)* as the mechanism that produces whisker formation and other blade deposits. However, the experimental data do not confirm this generalization. Taylor's data *(5)* also show that shear-thinning suspensions cause whiskers. Several works *(10–13)* provide examples of shear-thickening coatings that can be applied on pilot coaters. Huang *(1)* concludes that shear-thickening rheology alone is not a cause of runnability problems.

Flow instabilities have been identified as the mechanism behind coating streaks by Triantafillopoulos and Aidun *(14)*. This mechanism explains the large-scale nonuniformities of coat weight that can occur in the CD. However, this mechanism does not explain why an increase in the solids (an increase in viscosity and a decrease in Reynolds number) can lead to runnability problems. Obviously, there is another mechanism that leads to coating problems, and this mechanism is unrelated to flow instabilities.

Gane *et al.* *(6)* speculated that whiskering is a result of some sort of fracturing of the film between the filter cake and the blade at the exit. They discuss pressure dewatering and aggregation, but why these cause fracturing is not obvious. How to quantify this mechanism with a model is unclear.

Many papers in the literature discuss the importance of particle–particle interactions and the dewatering of the coating under the blade *(6, 15, 16)*. This dewatering of the coating and the subsequent buildup of a filter cake have been discussed for many years *(1, 10, 17)*. The rate of dewatering is recognized as an important parameter of a coating suspension, but only recently has this been studied in relationship to the filter-cake thickness during coating. Sandas *et al.* *(18)* describe an experimental technique to characterize dewatering rates. On-line dewatering rates can be obtained by the methods of Engstrom and Rigdahl *(19)* or Fujiwara *et al.* *(20)*. Letzelter and Eklund *(21, 22)* calculated filter-cake buildup at characteristic pressures and times during various stages of the coating process. In some cases, the dewatering was large and the filter-cake thickness was significant compared with the gap between the paper and the blade.

In the last 30 years, many models have been proposed to describe the blade-coating process. These have been summarized and discussed by Triantafillopoulos and Altug *(23)*, Roper and Attal *(13)*, and Pranckh and Scriven *(24)*. With the exception of Roper and Attal *(13)*, all of these models have assumed a Newtonian fluid. Chen and Scriven *(25)* account for the penetration of liquid into the porous substrate by postulating that the substrate deforms as it encounters forces. All of these models predict the blade force, but they do not take into account the influences of filter-cake formation or paper roughness. None of these models predict the onset of runnability problems.

In this paper, we propose a model for the blade-coating of paper that includes the formation of a filter cake on the base sheet. The impulse or pressure force is calculated from a mechanical-energy balance. The filter-cake thickness is calculated as a function of the local pressure field. The roughness of the paper is included in the model as the amount of coating taken up by the paper and thus removed from the fluid mechanics. For any given solids, dewatering characteristic, and blade geometry, the model predicts a maximum operating speed and a minimum coat weight. The model is compared with experimental data from several sources. This model represents the first attempt to include the dewatering of the suspension and the formation of a filter cake into the fluid mechanics.

The calculations quantify the balance between solids level, dewatering characteristics, and web velocities that must be obtained to have trouble-free coating. The model results give operational guidelines for blade-coating operations. The influence of thickeners, pigment-packing geometry, paper roughness, and coating viscosity on coater operations is quantified.

Model formulation

Geometry of modeled system

The model is concerned with the region just upstream of the blade and under the blade. **Figure 1** illustrates the general geometry of the situation. The thickness of the filter cake at any location x is designated $h_f(x)$. The distance between the average paper surface and the blade surface is denoted $h(x)$. The sheet can have any amount of roughness, but the model is concerned with the "average paper height," an issue that is discussed later. The filter-cake thickness increases in the x direction as liquid is driven from the coating. After the blade, the thickness of the filter cake continues to grow, but this does not influence the blade-coating operation. The filter cake moves at the same velocity as the web.

Assumptions

We do not need to worry about concentration gradients of solids in the bulk coating in this situation. In other words, we do not need to consider the concentration of solids at different thickness positions. When particles are carried to the paper interface or the filter-cake–coating interface, they will stay there because diffusion is small on the time scale of this process. Therefore, the solids in the liquid coating are the same as the application solids, and the solids in the filter cake will be some packing or maximum solids. Therefore, the filter cake has a sharp interface with the bulk coating, and we have only two solids concentrations in the problem.

The inlet thickness of the filter cake can be predicted using the technique of Letzelter and Eklund *(21, 22)* for a roll applicator or a short-dwell coater. The inlet pressure is taken to be the stagnation pressure from a mechanical-energy balance

$$P_{in} = \rho U^2/2 \qquad (1)$$

where

ρ = coating density

1. Geometry of the modeled system, with the distance between the web and the blade enlarged for illustrative purposes. The function $h(x)$ defines the distance between the web and the blade at any location, where $h(x)$ is measured from the average paper surface. The function $h(x)$ is input into the model and can describe different blade angles, geometries, or a deformed basestock. The function $h_f(x)$ denotes the filter-cake thickness at any location and is calculated in the model.

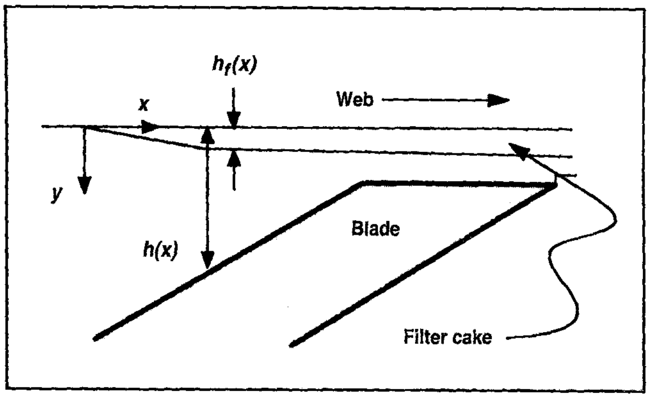

2. Schematic illustrating the effect of base-sheet surface roughness on the fluid-mechanics calculation. Coating that fills pores larger than pigment particles is removed from the calculation. Pores smaller than pigment particles receive liquid drained from the coating, leading to formation of a filter cake in localized areas above small pores. Much of the coating may not influence the critical limits, especially in lightweight coated paper.

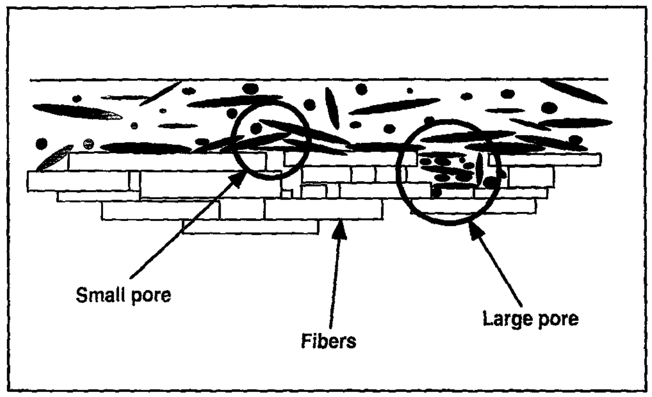

U = web velocity.

This corresponds to the "pressure plateau" of Pranckh and Scriven *(24)*, who found the stagnation pressure obtained from a mechanical-energy balance to be a good estimation of the pressure plateau just upstream of the blade heel. By taking this as the inlet pressure, the impulse force of Kahila and Eklund *(26)* should be correctly incorporated into the model *(23)*.

Other details of the model are described in the Appendix at the end of this paper, including the development of the lubrication approximation for the region just upstream of the blade and under the blade. The rate of filter-cake formation is also described in the Appendix.

Dewatering

Flow through a porous medium can be described by several relationships. The major resistance to flow in the case of paper coating is from the filter cake formed on the sheet surface. Using the nomenclature of Letzelter and Eklund *(21, 22)*, the mass flow rate per unit area is given by

$$m/f = C(\Delta P/h_f) \qquad (2)$$

where

m = mass flow rate of liquid from filter cake

f = filtration area

C = structure coefficient

ΔP = total pressure difference for dewatering between coating and paper web

h_f = thickness of filter cake.

The structure coefficient, C, is a function of the viscosity of the liquid, the particle shape, and the void fraction in the filter cake. The structure coefficient is the parameter that is determined in drainage experiments and is measured in units of seconds.

This structure coefficient plays a significant role in the model because it characterizes the rate of dewatering for a given coating. C should not be a function of solids, pressure difference, or the rate of dewatering. If C is large, the coating suspension does not form a filter cake that resists flow, and large dewatering rates can occur. If C is small, thin filter cakes strongly resist dewatering. C could be estimated from the liquid viscosity and from pigment shape and size.

The use of Eq. 2 to describe the rate of dewatering is based on Letzelter and Eklund's *(21, 22)* assumption that the rate of dewatering is controlled by the filter cake formed by the coating and not by the flow into the paper web. The pores in the paper web are large compared with the pores in the coating. (That is one reason why we coat paper.) Therefore, the limiting resistance to flow from the coating is the filter cake that is formed on the paper surface.

The working equations for the pressure profile and the filter-cake thickness are given in Eqs. 3 and 4, respectively.

$$\partial P/\partial x = \{Q-[U(h+h_f)/2]-(h_f U \phi_{max}/\phi)\}\,[12\mu/(h-h_f)^3] \qquad (3)$$

$$\partial h_f/\partial x = (C\Delta P/U\rho_l h_f)\,[\phi/(\phi_{max}-\phi)] \qquad (4)$$

Both equations are developed in the Appendix.

The inlet pressure is defined in Eq. 1. The exit pressure is taken to be atmospheric pressure. Q, the volumetric flow rate of coating per unit width, is related to the coat weight and is described in the Appendix. The ΔP term in Eq. 4 describes the hydrostatic pressure but also includes capillary pressure (or sorption potentials) and the pressure of air trapped inside the web. Note that at high solids, the filter-cake thickness can grow rapidly because less water needs to be removed to cause the same amount of filter-cake growth. As the web velocity increases, the time for dewatering decreases and therefore the time for filter-cake growth decreases. However, an increase in web velocity increases the impulse pressure and the pressure pulse under the blade nip. As the filter-cake thickness grows, the rate of dewatering decreases. C becomes the major "controllable" parameter influencing the amount of dewatering.

Computation techniques

Equations 3 and 4 are two first-order differential equations that can be solved with finite-difference techniques. A number of numerical methods are possible, but one simple procedure is as follows:

1. Select a reasonable value of Q, the volumetric flow rate.
2. Integrate the pressure and filter-cake expressions (Eqs. 3 and 4) with Euler's method starting at $x=0$
3. If the pressure at the blade exit is atmospheric, then the solution is found. If not, adjust the value of Q and integrate again.
4. Once the pressure boundary conditions are met, calculate normal and tangential forces on the blade (Eqs. A9 and A10 in the Appendix).

There are certain techniques to adjust Q. Newton's method has quadratic convergence if the solution is stable. Boundary-value finite-difference techniques can solve the problem without a trial-and-error method. A typical run on a 486 personal computer takes 10 s to find a solution. Critical conditions, such as when the filter cake is near the blade surface, can take more computer time. The normal and tangential forces on the blade are calculated as described in the Appendix.

The initial value of h_f must be provided to cause the derivative in Eq. 4 to be finite at $x = 0$. A small value of 0.2 μm is used in all cases in the present work. This initial value could be calculated by the methods of Letzelter and Eklund *(21, 22)* to include the effect of a roll applicator or the dewatering in the pond.

If deformation of the blade or the base sheet is of interest, another iteration can be placed in the program. Once the pressure profile is obtained for a given geometry, the blade and paper profiles can be adjusted to match this new pressure profile. This will modify the gap between the blade and the filter cake. Therefore, the calculation can be repeated until convergence. The effects of running the blade at different angles (on the heel or toe) or of running a worn blade are easily investigated by the input for $h(x)$, the distance from the sheet to the blade.

Dimensionless parameters

Four dimensionless parameters become important in this model.

Pressure. If pressure is made dimensionless with $\mu U/l$, then the dimensionless inlet pressure becomes

$$P^*_{in} = \rho U l / 2\mu$$

The variable l is an arbitrary characteristic length of the problem and is taken as 1.0 mm here, a selection that does not influence the results. Thus as web speed increases, the pressure plateau increases, driving more liquid from the coating.

ϕ/ϕ_{max}. The volume ratio of applied coating solids and filter-cake solids, ϕ/ϕ_{max}, is a very important parameter. As this ratio approaches one, the filter cake grows rapidly with a small amount of water loss.

Rate of water loss. The parameter for the rate of water loss, C, is made dimensionless with viscosity and density of the coating suspension

$$C^* = C\mu/\rho l^2$$

The viscosity used here is the viscosity of the coating suspension and not the viscosity of the liquid phase. The value of C may change as thickening agents are used, but the value of the suspension viscosity, μ, will also increase. If these changes are of the same order of magnitude, the use of a thickening agent will not affect the value of C^*.

Sheet roughness. The fourth important parameter is the paper roughness or volumetric surface roughness. This represents the amount of coating instantaneously taken up by the paper and removed from the fluid mechanics of the coating process. The surface roughness consists of pores or pockets that are greater in length than the pigment of interest. This concept was proposed by Kahila and Eklund *(26)* and Eklund *(27)*. Pores that are smaller than the pigment will be the regions that take up liquid and form a filter cake.

Figure 2 illustrates the concept of sheet roughness. Pores that are smaller than the average pigment size remove liquid from the coating, causing a filter cake to form. Pores that are larger than the average pigment size "remove" coating from the fluid mechanics and do not cause a filter cake to form above the average paper surface.

This concept of roughness can be included in the model by adjusting the target coat weight in the fluid mechanics. For example, if 20 g/m² is the wet coat weight but 5 g/m² is hidden from the fluid mechanics because of large pores, then the target coat weight is 15 g/m² on a smooth paper surface. This point can be refined as details with regard to the paper substrate are known.

The paper roughness (the number of large pores) will play a greater role in lightweight coated papers, where target coat weights are low. Localized areas of high solids can form and cause localized thick filter cakes. The model is concerned with these localized areas of dewatering, not the entire paper sheet. The area above the large pore in Fig. 2 will not cause doctoring problems. It is the area above the small pore that has potential to cause problems during the blade-coating process. Figure 1 should be understood to

3. The pressure pulse developed under a blade for the base-case conditions of Pranckh and Scriven *(24)*. The data points were adjusted upward by 60 units to cause the exit pressure to be zero, the same as in the model.

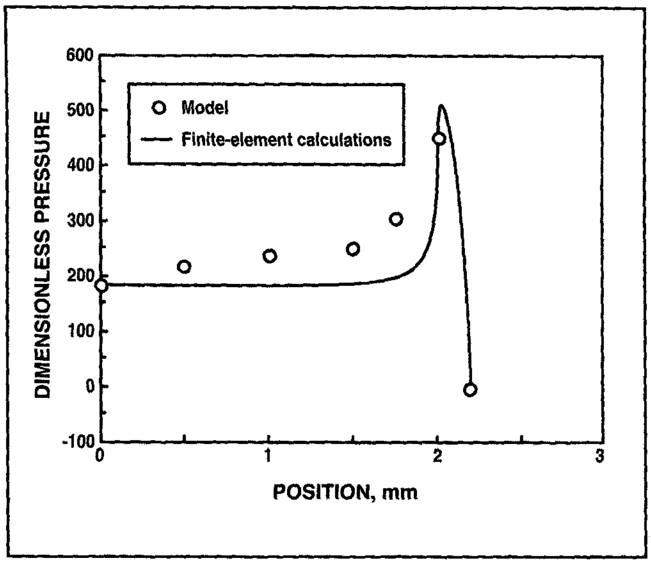

4. Pressure profiles calculated by the model for cases where the blade is run on the toe (positive pressure) and on the heel (negative pressure) for the base-case conditions of Pranckh and Scriven *(24)*.

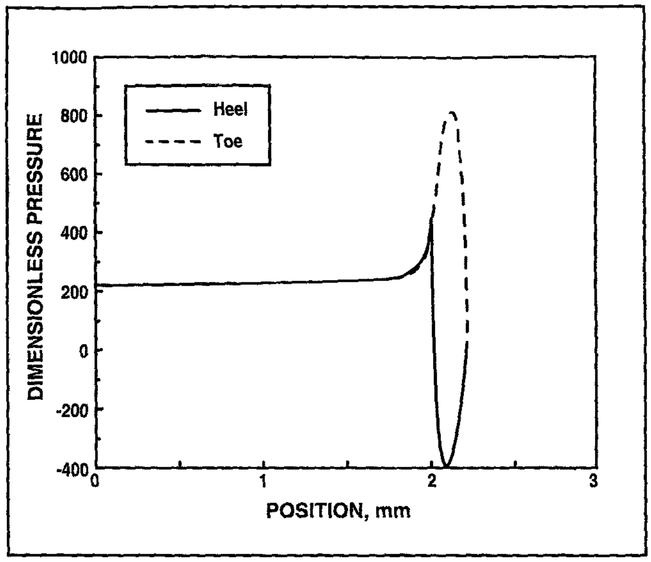

represent only the critical regions. We are concerned only with localized regions that dewater and form a filter cake.

Rheology

Most coating suspensions are non-Newtonian, exhibiting shear-rate-dependent viscosities and time-dependent properties (viscoelasticity). The numerical method of Scheller *(28)* could be used to handle viscosities that depend on shear rate (either shear thinning or shear thickening). Viscoelastic properties would likely need to be incorporated into finite-element techniques. However, the framework presented in this work could be used with these other rheological models to predict the limits for web velocity and coat weight.

Model results

The approximations in the model's fluid mechanics do not appear to compromise the results. For example, with no liquid absorption ($C = 0$) and a smooth paper surface, we obtain pressure-pulse results that are very similar to those of Pranckh and Scriven *(24)*. **Figure** 3 compares the model predictions with their base case (U = 15 m/s, μ = 0.05 Pa·s, ρ_l = 1200 kg/m^3, 0.206-mm blade thickness, and the gap as reported in their Fig. 3). Pressure is made dimensionless with $\mu U/l$, where μ is the viscosity of the coating suspension and l is some length. The results from the two-dimensional finite-element calculation are the data points in Fig. 3 [taken from Fig. 5 in Pranckh and Scriven *(24)*]. These results include the inertial terms of the Navier–Stokes equations. The length scale is taken to be 1 mm. Therefore, the dimensionless pressure values are a factor of 10 higher than reported in Pranckh and Scriven *(24)*. In addition, the exit pressure is zero in our model. Therefore, the data points from the finite-element method are adjusted upward by a value of 60 units to match this exit pressure condition. This shift made many of the finite-element results larger than the current model in the stagnation region. As Fig. 3 shows, the model predicts the correct magnitude of pressure at every location, though there are some differences. The peak of the pressure pulse is larger, and the pressure pulse builds more rapidly in our model compared with the finite-element results. Using the stagnation pressure to calculate the inlet pressure 2 mm in front of the blade gives good results.

The model also provides the same types of pressure profiles as Pranckh and Scriven *(24)* obtained for the blade running on the heel or the toe. The pressure profiles are in **Fig. 4.** The broken line in Fig. 4 is the case for running on the toe. For the case when the blade runs on the heel (the solid line), there is a large negative pressure generated under the blade. These modeled results were obtained using the same base-case conditions as in Fig. 3, but with the data for the blade adjusted to simulate a diverging nip (run on heel) or a converging nip (run on the toe). In practice, the blade would rapidly wear to form a parallel channel, but the modeled results confirm the validity of the fluid-mechanics calculations.

When water migrates from the coating layer into the paper web, a filter cake forms on the sheet surface. At a given coat weight, the gap between the top of the filter cake and the blade surface decreases, thus increasing the force on the blade. At some critical conditions, the filter-cake thickness becomes significant, and the pressure pulse also in-

5. Calculated normal force for different coat weights. For no dewatering ($C = 0$), any coat weight can be obtained. For measurable dewatering ($C = 7.25 \times 10^{-12}$ s), the force rapidly goes to large values at a wet-coat thickness of 6.45 μm. This correlates to the condition of excessive filter-cake growth.

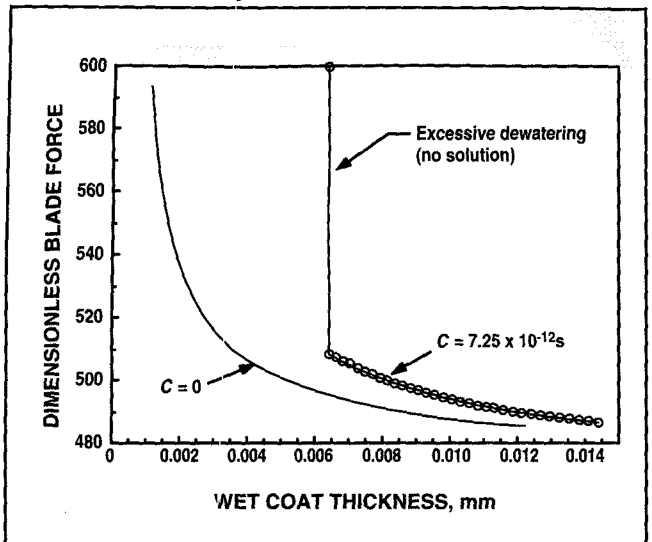

6. Dewatering under the blade. The converging gap between the top of the filter cake and the blade in the right-hand figure creates a large pressure pulse. This pressure pulse promotes dewatering even further and excessive filter-cake growth.

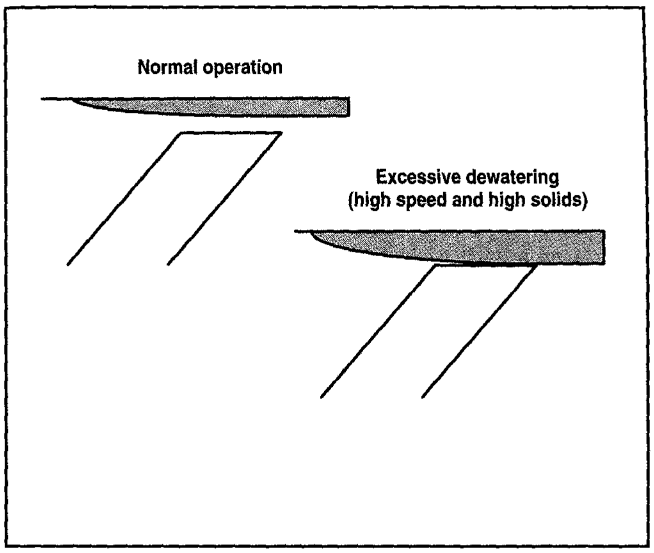

creases, which drives more liquid into the web. The normal force goes to large values, and the model cannot find a solution to the equations. This is illustrated in **Fig.** 5 for values of U = 1000 m/min, μ = 0.05 Pa·s, blade angle = 45°, blade thickness = 0.2 mm, a stagnation pressure at 2 mm before the blade, and an entrance length of 10.0 mm. The density of the liquid phase, ρ_l, is 1200 kg/m³. Force is made dimensionless with the group μUl. The solid line is for $C = 0$ (no dewatering), and the broken line is for $C = 7.25 \times 10^{-12}$ s. The volume ratio of solids, ϕ/ϕ_{max}, is 0.9. With no water absorption, the coat weight can be adjusted to very low values by increasing the blade force. However, when C is any finite value, there is a point where the force drastically increases. This defines the location of minimum coat weight that can be obtained. In addition, this can be thought of as the maximum speed that can be used to obtain that given coat weight.

Even with no paper roughness or instantaneous coating penetration included in the model, there is a maximum speed and a minimum coat weight for a given set of conditions. The minimum coat weight corresponds to the maximum that can be removed by the blade without generating too much pressure. The maximum speed corresponds to the impulse pressure generated before the blade that does not produce excessive filter cake. The physical situation is depicted in **Fig. 6.** Under normal operations, the filter-cake thickness is less than 2 μm. However, at high speeds and solids, the filter cake grows to a value that is comparable with the distance between the paper and the blade. This causes excessive pressure pulses that drive even more liquid into the web.

Figure 7 shows the maximum velocity–minimum coat weight predicted by the model for the same conditions as given in Fig. 5 (smooth sheet with no surface roughness, $C = 7.25 \times 10^{-12}$ s, and $\phi/\phi_{max} = 0.9$). These results are given in the upper curve. The lower curve depicts results for $\phi/\phi_{max} = 0.8$. In both cases, lower coat weights can be obtained at lower web speeds because of the smaller dewatering pressures in the blade nip. Velocity–coat-weight combinations that are to the left of or above the lines are possible. Combinations to the right of or below the lines are not obtainable because of excessive dewatering.

The lines in Fig. 7 depict well-known results and can be used as operational guidelines. If a coating is operating well and providing a target coat weight at a given solids–speed combination, an increase in speed can lead to runnability problems. For example, Point A represents a coat thickness of 6 μm at a web velocity of 500 m/min and a solids level that gives a volume ratio of solids (ϕ/ϕ_{max}) of 0.9. Point B represents the same conditions but at a web velocity of 1000 m/min. At this speed, the coating no longer runs well, as indicated by its position below the line for $\phi/\phi_{max} = 0.9$, which is a position of excessive filter-cake growth. If the solids level of the coating is reduced so that $\phi/\phi_{max} = 0.8$, the new line is located below Point B, which places Point B in a region that corresponds to low filter-cake growth (compared with the blade gap).

Given the quality and efficiency benefits of running at high solids, it is important to know where the operational condition falls on a figure like Fig. 7 for any given paper–coating combination. If the location is

7. The calculated critical combinations of velocity and coat weight for the same conditions as in Fig. 5, with $C = 7.25 \times 10^{-12}$ s. Coat-thickness–web-velocity combinations located beneath the applicable curve are not possible because of excessive dewatering.

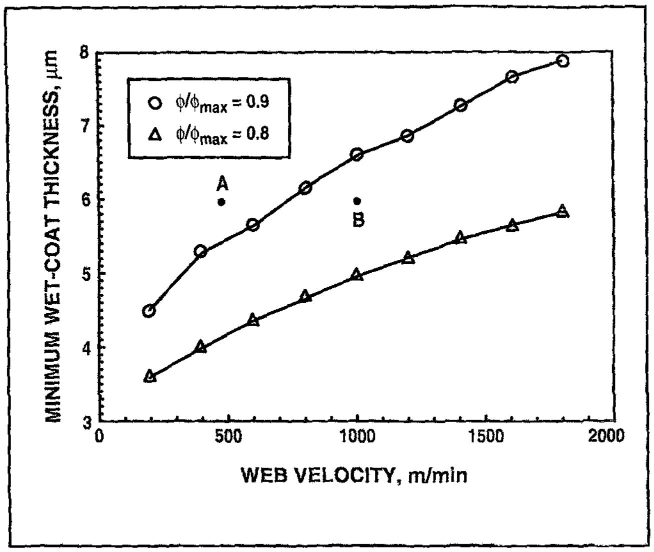

8. Comparison with data from Kuzmak *(29)*. The normal force from the model is converted to gauge pressure by fitting the values of the data. The left-hand end of the solid lines represents the minimum coat weight possible.

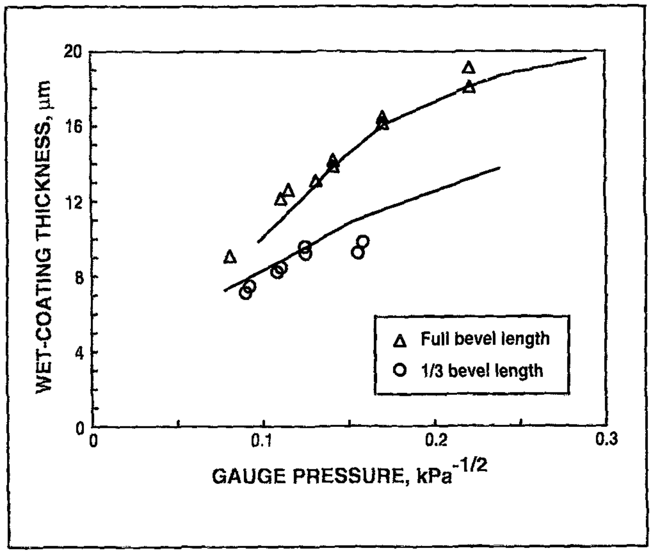

far to the left of or above the line, the solids level or the velocity can and should be increased to optimize quality and minimize costs. If the conditions are near the line, the coating is operating at its threshold and no changes can be made. Efficient operations occur above the line but as close to the line as possible.

The *opposite* results from Fig. 7 are obtained for some roll applicator systems. When a significant proportion of the dewatering occurs between the roll applicator and the blade, a thick filter cake will form for the inlet conditions of the model. The inlet filter-cake thickness is proportional to one over the square root of the web velocity. Therefore, as the web velocity decreases, a larger filter cake forms at the inlet, which sets a lower bound to velocity for a given target coat weight. As the web velocity increases, there is less time available for dewatering, so lower coat weights are possible. In this case, lines would have the opposite slope compared with Fig. 7.

Kuzmak *(29)* compared blade tube pressures with different blade geometries for different coat weights. The gauge pressure reported is difficult to compare with the force calculated in our model because details with regard to the area of the tube pressing against the blade and the forces supported by the blade holder are not known. However, the data are in the range where the tube pressure does influence the coat weight. The minimum coat weight is reported for two different blade geometries, with one blade having a land area one-third of the other. The application solids was 60%, which gives a solids volume fraction of 0.42. The coating viscosity, μ, was 0.044 Pa·s at a shear rate of 45,900 s^{-1}. The machine speed was 610 m/min. If the filter-cake volume fraction is 0.58, the volume fraction ratio is 0.73. Assuming an entrance length of 2 mm, a blade angle of 45°, and the standard blade to have a thickness of 0.3 mm, a value of $C = 2.5 \times 10^{-11}$ s gives the results in **Fig.** 8. This value of C is about a factor of ten larger than the base-case value used in Letzelter and Eklund *(21, 22)*, but the required value of C will decrease if we decrease the target coat weight to account for paper roughness. Therefore, this value of C is reasonable for our purpose at present. The normal force calculated from the model was converted into the tube pressure by subtracting a value near the impulse force (to account for the blade support) and finding a factor that matched the reported gauge pressure in the mid region of the data. Therefore, the model gauge pressure values should not be taken as absolute calculated quantities but as fitted quantities. However, the model does distinguish between the two different blade geometries and predicts the minimum coat weight for both with a single value of C.

Taylor *(5)* provided data for the maximum web velocity that can be obtained before whiskers were observed. The blade thickness was 0.3 mm, the blade angle was 45°, and the blade extension was 57 mm. The viscosities of the coatings were reported for every solids level. The open circles in **Fig. 9** represent the web velocities at which whiskers were observed at each solids level for the last coating formulation in Taylor's Table II (No. 2 clay and no latex). The solids levels in Taylor's data were converted to volume fraction assuming a solids density of 2000 kg/m^3. The squares in Fig. 9 represent the modeled results assuming that the volume fraction of solids in the filter cake is 0.58, the target wet-

9. The velocity for whisker formation as a function of coating solids for published data *(5)* and as predicted by model, with *C* adjusted to 4 x 10^{-12} s

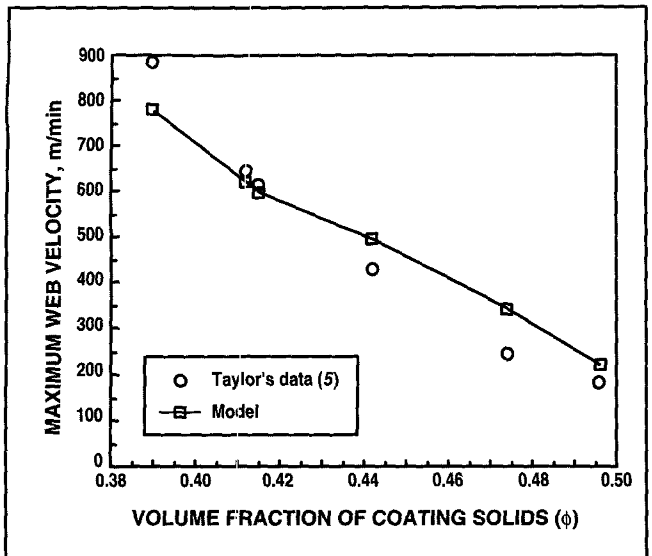

10. Decrease in maximum web velocity with increasing coating solids for published data *(6, 7)* and as predicted by model

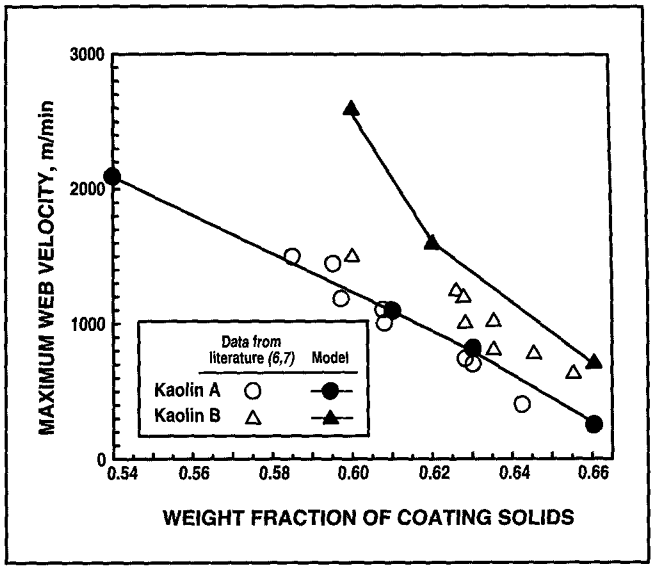

coat thickness is 9 µm, and C = 4 x 10^{-12} s. Using the viscosities reported by Taylor at each solids level, the model produces a unique prediction for maximum web speed at each level of coating solids. These predictions are in agreement with Taylor's data. The value of *C* was adjusted downward for the cases where thickener was added. The proportion of downward adjustment was as suggested by Darcy's law. The value of *C* used in the model is well within reason when the target coat weight is low (to account for coating absorbed by large pores; the actual coat weight can be much larger). Though there are two parameters that were adjusted, the model correctly captures the trends in the data. Adjustment of these two parameters only influences the magnitude of the numbers, not the slope of the line.

The data of Gane *et al. (6)* and McGenity *et al. (7)* included dewatering rates, which allows calculation of *C*. For the kaolin identified as Alphaplate (Kaolin A) and SPS (Kaolin B), 110 g/m² and 50 g/m² were collected in 50 s at 0.25 bar of pressure, respectively. This gives values of *C* of 3.14 x 10^{-11} s and 6.6 x 10^{-12} s for Kaolins A and B, respectively.

I. Viscosity and solids fractions for coatings containing Kaolins A or B[a]

Kaolin type[b]	Weight fraction of coating solids	Volume fraction of coating solids (ϕ)	ϕ/ϕ_{max}[c]	Coating viscosity (µ), Pa·s
A	0.54	0.37	0.63	0.01
A	0.61	0.44	0.76	0.03
A	0.63	0.46	0.80	0.05
A	0.66	0.49	0.86	0.08
B	0.60	0.43	0.74	0.03
B	0.62	0.45	0.79	0.05
B	0.66	0.51	0.87	0.10

[a]Data from Gane *et al. (6)* and McGenity *et al. (7)*
[b]Kaolin A is a delaminated clay (Alphaplate) from the United States; Kaolin B is an English coating clay (SPS).
[c]The volume fraction of solids in the filter cake, ϕ_{max}, is assumed to be 0.58.

The last value is close to the suggested value of Letzelter and Eklund *(21, 22)* of 7.25 x 10^{-12} s. The value of *C* should not be a function of the solids content. The smaller value of *C* for Kaolin B indicates a coating with good water-holding ability. The high-shear-rate viscosity reported by Gane *et al. (6)* and McGenity *et al. (7)* for the coatings at various solids are given in **Table I.** The maximum volume fraction or the volume fraction in the filter cake is taken to be ϕ_{max} = 0.58 for both cases. The actual value could be obtained with a simple experiment.

The inlet pressure is taken to occur 2 mm upstream of the blade heel in all cases. The inlet filter-cake thickness is assumed to be small but finite, with a value of 0.2 µm. The roughness and porosity of the paper used in the experiments is not known. Therefore, the amount of coating "removed" from the fluid mechanics is unknown. The target coat weight for the coating containing Kaolin B is adjusted to give a reasonable result. This adjustment affects the vertical position of the line but not the line's slope. The lines and the filled symbols in **Fig. 10** show the result when the target wet-coat thickness is 7 μm and 5 μm for Kaolins A and B, respectively. The actual coat weights were not reported in the work. However, if half of the coating is taken up by pores in the sheet surface, this would result in reasonable coat weights.

The model describes the correct slope of the data. In addition, the model distinguishes between the two different pigments even if the same target coat weight is used. The Kaolin B, which had a slower dewatering characteristic compared with the Kaolin A, has a higher speed limit. The value of the structure parameter C is critical to obtain good runnability limits at high solids. C should be as small as possible to prevent rapid filter-cake formation.

If the same target wet-coat thickness is used, say 7 μm, the model overpredicts the maximum velocity of the Kaolin B system by 1000 m/min. The reason for this is not certain. If the maximum volume fraction of the B system is lower than 0.58, e.g., at 0.54, then the same target coat weight would predict both pigment systems. A number of other variables may be at play here also. The runnability problems with the B system may be related to flow instabilities, air entrapment, or other coat-weight control issues at high speeds. However, this first modeling attempt seems promising in quantifying such runnability limits.

Conclusions

The proposed model is the first to incorporate the formation of a filter cake and dewatering into the fluid mechanics of blade coating. Sheet roughness and porosity are included in the model as locations that remove coating volume from the fluid mechanics computations. The impulse force or inertial effects are included as an inlet-pressure boundary condition. The velocity profile, pressure pulse, filter-cake thickness profile, and final coat weight are predicted by the model given the web velocity, coating density and viscosity, blade geometry, and the dewatering properties of the coating.

For a smooth paper web with no water removal, the fluid mechanics are similar to those reported in the literature. The impact pressure and the pressure pulse are calculated by the model, which predicts a negative pressure pulse under the blade when the blade is running on the heel.

The coating's solids level and its dewatering properties determine the maximum web velocity for a given coat-weight target. When the filter-cake thickness approaches the same order of magnitude as the blade gap, large pressure pulses develop. This drives more liquid from the coating suspension into the sheet.

The model predicts critical operating conditions for given solids contents and web velocities. Results from the model show similar trends as data from the literature, indicating that the model can be used to establish operational guidelines.

Literature cited

1. Huang, D. K., *TAPPI 1986 Blade Coating Symposium*, TAPPI PRESS, Atlanta, p. 175.
2. Van Gilder, R. L. and Purfeerst, R. D., *TAPPI 1986 Coating Conference Proceedings*, TAPPI PRESS, Atlanta, p. 45.
3. Toivakka, M., Eklund, D., and Bousfield, D. W., *TAPPI 1992 Coating Conference Proceedings*, TAPPI PRESS, Atlanta, p. 403.
4. Kuang, S. J., Ferguson, C. A., Rezanowich, A., *et al.*, *Tappi J.* 67(8): 86(1984).
5. Taylor, J. A., *TAPPI 1987 Coating Conference Proceedings*, TAPPI PRESS, Atlanta, p. 1.
6. Gane, P.A.C., McGenity, P. M., and Watters, P., *Tappi J.* 75(5): 61(1992).
7. McGenity, P. M., Gane, P.A.C., Husband, J. C., *et al.*, *TAPPI 1992 Coating Conference Proceedings*, TAPPI PRESS, Atlanta, p. 133.
8. Tran, T. H., Coco, C. E., and Dill, D. R., *TAPPI 1993 Coating Conference Proceedings*, TAPPI PRESS, Atlanta, p. 51.
9. Engstrom, G. and Rigdahl, M., *TAPPI 1989 Coating Conference Proceedings*, TAPPI PRESS, Atlanta, p. 59.
10. Bohmer, E., *Norsk Skogind.* 21(8): 258(1967).
11. Canard, *Tappi* (53):(1970).
12. Windle, W. and Beazley, K. M., *Tappi* 50(1): 1(1967).

Nomenclature

C	=	structure parameter
CW	=	coat weight
f	=	filtration area
F_n	=	normal force on blade per unit width
F_t	=	tangential force on blade per unit width
h	=	distance from sheet (average height) to blade
h_f	=	distance from sheet (average height) to top of filter cake
l	=	characteristic length (1 mm here)
L	=	length of region from inlet to blade exit
m	=	mass of liquid removed from coating layer
P	=	pressure at any x position
P_{in}	=	inlet pressure
ΔP	=	total pressure difference for dewatering between coating and paper web
Q	=	volumetric flow rate per unit width
U	=	web velocity
v	=	velocity in x direction
x	=	machine-direction coordinate
y	=	normal direction to paper coordinate
μ	=	viscosity of coating suspension
ρ	=	density of coating suspension
ρ_p	=	density of particles in coating suspension
ρ_l	=	density of liquid in coating suspension
ϕ	=	volume fraction of solids in coating suspension
ϕ_{max}	=	volume fraction of solids in filter cake

Appendix: Model mathematics

The fluid mechanics just upstream of the blade nip and under the blade is described by the lubrication approximation. The inertial terms or the impact force are accounted for by the inlet pressure calculated as the stagnation pressure. The Navier–Stokes equations become

$$\partial P/\partial y = 0 \quad \text{(A1)}$$

$$\partial P/\partial x = \mu(\partial^2 v/\partial y^2) \quad \text{(A2)}$$

where P is the pressure, μ is the viscosity of the coating suspension, and v is the x-directed velocity. Note that Eq. A1 shows that pressure is not a function of the y coordinate. The results of Pranckh and Scriven *(24)* contain mostly vertical isopressure lines for many conditions in this region, indicating that the lubrication approximation is valid near the blade entrance and under the blade. Thus the lubrication approximation should contain the correct physics while producing a fluid-mechanics-based model that is computationally simple. The magnitude and detail of the flow field upstream of the blade may not be quantitatively correct, but the critical region where the pressure pulse occurs is correctly modeled.

The velocity profile is obtained by integrating Eq. A2 with respect to the y coordinate and applying the following boundary conditions:

$$\text{at } y = h_f(x),\ v = U$$

$$\text{at } y = h(x),\ v = 0$$

Both boundary conditions represent the no-slip conditions at the filter-cake–coating interface and at the blade–coating interface. The velocity profile at any x position is

$$v = \{[U(h-y)]/(h-h_f)\} + \{(\partial P/\partial x)\,[(y^2-yh-yh_f+hh_f)/2\mu]\} \quad \text{(A3)}$$

The continuity equation can be manipulated to give

$$Q = \int_{hf}^{h} v\,dy + h_f U(\phi_{max}/\phi) \quad \text{(A4)}$$

where Q is the volumetric flow rate per unit width for any vertical slice, and ϕ_{max} and ϕ are the volume fraction of solids in the filter cake and in the coating, respectively. The first term, the integral, represents the flow rate between the filter cake and the blade. The second term is the volumetric flow rate of coating contained in the filter cake. The term $h_f U$ is the volumetric flow rate of the filter cake per unit width. When this is multiplied by the ratio ϕ_{max}/ϕ, the quantity becomes the volumetric flow rate of the initial coating suspension represented by the filter cake. This volumetric flow rate needs to be constant for any vertical slice and is related to the coat weight applied to the paper.

The coat weight (mass per unit area) is obtained as

$$\text{CW} = Q\phi\rho_p/U \quad \text{(A5)}$$

where ρ_p is the density of the solids.

When the velocity profile is inserted into the continuity equation, the result can be rearranged to give

$$\partial P/\partial x = \{Q-[U(h+h_f)/2]-(h_f U\phi_{max}/\phi)\}[12\mu/(h-h_f)^3] \quad \text{(A6)}$$

The filter-cake thickness is a function of the mass of liquid that has drained through the filter cake. From a material balance, the following relationship is obtained between the filter-cake thickness and the mass of liquid drained

$$h_f = (m/f\rho_l)\,[\phi/(\phi_{max}-\phi)] \quad \text{(A7)}$$

where ρ_l is the density of the liquid and m is the mass drained through the filter cake. This expression accounts for the mass of liquid still inside the filter cake, i.e., the liquid in the filter-cake pores. As the volume fraction of coating solids approaches the volume fraction of filter-cake solids, it takes very little liquid removal to increase the filter-cake thickness. Using Eqs. 2 and A7 and replacing the time derivative of m with a spatial derivative, the filter-cake thickness will grow according to the following relationship

$$\partial h_f/\partial x = (C\Delta P/U\rho_l h_f)\,[\phi/(\phi_{max}-\phi)] \quad \text{(A8)}$$

Equations A6 and A8 are the working equations of the model.

Once the pressure profile and the filter-cake profile are obtained, the velocity profile at any position can be calculated with Eq. A3.

The normal force on the blade per unit width is calculated as

$$F_n = \int_0^L P\,dx \quad \text{(A9)}$$

where F_n is the normal force and L is the total length in the x direction.

The tangential force F_t per unit width is found as

$$F_t = \int_0^L -\mu(dv/dy)dx \quad \text{(A10)}$$

The derivative needs to be evaluated at the blade surface (at $y = h$). Therefore, the derivative of Eq. A3 is taken with respect to y and evaluated at $y = h$. The pressure gradient at every x location is known. Therefore, the velocity gradient at the blade surface is calculated at every x location. The integration in both cases is done using a standard numerical technique.

13. Roper, J. A. and Attal, J. F., *Tappi J.* 76(5): 55(1993).
14. Triantafillopoulos, N. and Aidun, C. K., *Tappi J.* 73(6): 127(1990) [correction 73(8): 16(1990)].
15. LePoutre, P., *The structure of paper coatings: an update,* TAPPI PRESS, Atlanta, 1990.
16. Branston, R. E., Clark, P. C., Errico, M., *et al., TAPPI 1993 Coating Conference Proceedings*, TAPPI PRESS, Atlanta, p. 79.
17. Follette, W. J. and Fowells, R. W., *Tappi* 43(11): 953(1960).
18. Sandas, S. E., Salminen, P. J., and Eklund, D., *Tappi J.* 72(12): 207(1989).
19. Engstrom, G. and Rigdahl, M., *TAPPI 1985 Coating Conference Proceedings*, TAPPI PRESS, Atlanta, p. 35.
20. Fujiwara, H., Fujisaki, N., and Kaga, C., *TAPPI 1991 Coating Conference Proceedings*, TAPPI PRESS, Atlanta, p. 179.
21. Letzelter, P. and Eklund, D., *Tappi J.* 76(5): 63(1993).
22. Letzelter, P. and Eklund, D., *Tappi J.* 76(6): 93(1993).
23. Triantafillopoulos, N. and Altug, N., *AIChE 1991 Forest Products Symposium Proceedings*, TAPPI PRESS, Atlanta, p. 141.
24. Pranckh, F. R. and Scriven, L. E., *Tappi J.* 73(1): 163(1990).
25. Chen, K. S. A. and Scriven, L. E., *Tappi J.* 73(1): 151(1990).
26. Kahila, S. J. and Eklund, D. E., *Wochbl. Papierfabr.* 106(17): 661(1978).
27. Eklund, D. E., *TAPPI 1984 Coating Conference Proceedings*, TAPPI PRESS, Atlanta, p. 37.
28. Scheller, B. L., "Drop formation and the spreading behavior of Newtonian and shear-thinning liquid drops impacting a solid surface," Ph.D. thesis, University of Maine, Orono, 1993.
29. Kuzmak, J. M., *Tappi J.* 69(2): 72(1986).

We would like to thank the industrial sponsors of the University of Maine Paper Surface Science Program and a grant from the TAPPI Foundation. P.A.C. Gane provided viscosity information. P. LePoutre contributed useful discussions.

Received Dec. 2, 1993.

Accepted Jan. 12, 1994.

Presented at the TAPPI 1994 Coating Conference.